Journal of Positive Sciences (JPS) eISSN: 2582-9351, https://positive-sciences.com JPS. 2026 May; 6(3): 20-30

Article info
Received on: 02.03.2026
Accepted on: 07.04.2026
Published on: 11.05.2026
doi: https://doi.org/10.52688/ASP58267

Research Article

Eco-Friendly Extraction of Nano-Activated Carbon as A Potent Reinforcement For Al7075 Alloy, A Mechanical And Wear Analysis: Promote A Sustainable Environment

Ruaa A. Salman[1,*]

[1] College of Biomedical Engineering, University of Technology-Iraq

[*] 70153@uotechnology.edu.iq

ABSTRACT

This study aims to find an ecological and high-performance solution to produce high-performance Al7075 matrix nanocomposites with the use of bio-sourced reinforcements. A major achievement in this study is that agricultural biomass (cotton carpel) was converted into high-grade Nano-Activated Carbon (NAC) using a controlled thermochemical heating process, hence providing an ecological option for synthetic carbon-based materials. The synthesized NAC particles were incorporated into the aluminum matrix at 3 different weight fractions (0.1, 0.2, and 0.3 wt.%) using the stir casting technique, and their microstructure and mechanical properties were evaluated using Vickers microhardness and wear testing under 3 different load settings (5N, 10N, and 15N). Results showed that the addition of NAC acted as a strong strengthening agent and resulted in an increase in microhardness of the 0.3 wt.% NAC composite from 130 HV for the base alloy to 164 HV. This mechanical enhancement can be explained by a wear-strengthening mechanism, where the uniform distribution of NACs hinders dislocation movement. The results of the tribological tests showed that the 0.3 wt.% NAC composite had a maximum 90.72% higher wear resistance when compared to the base alloy at 15N. The optical micrographs of the wear surfaces show that the cast alloy had severe delamination and abrasive plowing, but with the arrival of the nanocomposites, there was a smooth, or protected, surface due to the formation of a stable tribological layer. This result validates that nanocarbons made from recycled resources provide significant performance advantages over nanocarbons derived from traditional (synthetic) sources in their utility as reinforcement materials for the construction and production of advanced metallic composite materials. These materials provide a sustainable engineering alternative that offers both low-density constructions along with superior strength and durability (ability to withstand wear) properties and are, therefore, well suited for use in industrial applications requiring large quantities of materials subjected to very high levels of repeated fatigue loading.

Keywords: Al7075 alloy, Nano-activated carbon (NAC), Biomass valorization, Stir casting, Microhardness, Wear strengthening

INTRODUCTION

A paradigm shift towards “green metallurgy” in conjunction with a “circular economy” is currently taking place in the industrial world, due to the need to reduce environmental impacts caused by agricultural waste and depleting non-renewable mineral resources. Every year, there are billions of tons of lignocellulosic biomass is generated by agriculture [1]. These lignocellulosic biomass sources include rice husks, coconut shells, oil palm empty fruit bunches (EFB), and more energy dense biomass such as cotton carpel [1-4]. The majority of these types of biomass are typically underutilized, unnecessarily disposed of in environmentally hazardous ways (such as open field burning) or currently regarded as waste. Doke and Khan (2017) [1] state that these lignocellulosic biomass residues are not simply waste, but rather carbon-rich precursors to high value Nano-Activated Carbon (NAC) that can be created using thermochemical processing techniques [3]. In creating NAC, there are two major processing steps: carbonization and activation [5]. Ahmad and Alrozi (2011) [2] state that the carbonization step is where the lignocellulosic biomass undergoes thermal decomposition in an inert atmosphere to remove volatile compounds from the sample, which produces a carbonaceous skeletal structure. After the carbonization process has occurred, chemical activation occurs using chemical activators (KOH, $ZnCl_2$, H_3PO_4) and creates a complex system of micropores/mesopores that dramatically increase the surface area (typically 1000 m^2/g or greater) of the NAC. The introduction of nanomaterials has fundamentally changed the definition of material science [3-6]. Nanomaterials have a minimum of one dimension within the 1-100 nm range, possess unique physical, chemical, and mechanical properties that are dramatically different from their bulk form due to the size effect caused by both high surface area to volume ratio and quantum confinement effects [4]. Nanomaterials have become the foundation for Industry 4.0, i.e., the Fourth Industrial Revolution, in relation to industrial applications [6-8]. These materials will play a crucial

*Corresponding author
Ruaa A. Salman,
College of Biomedical Engineering, University of Technology-Iraq
e-mail: 70153@uotechnology.edu.iq

role in numerous industries, including energy storage (supercapacitors and batteries), environmental pollution control, high-performance engineering, and more. Their application in medical fields, particularly dental fillings, will create a significant transformation [9]. In other words, the shift from micro-fillers to nano-fillers enables the development of "smart materials" capable of performing multiple functions, such as self-sensing, high thermal stability, and exceptionally high strength-to-weight ratios [10]. In the metallurgical industry, the incorporation of carbon nanoparticles into metal networks has become essential to meet the stringent specifications of next-generation components in the aerospace and automotive industries [11]. Historically, carbon fillers have been used in products such as carbon black in polymers, primarily to enhance rubber's UV resistance, electrical conductivity, and weathering properties [12, 13]. According to Spathis and Kontou [4], the shape and surface activity of the carbon particles determine the viscoelastic properties of polymer composites; however, the modern-day challenge is to develop metal matrix nanocomposites (MMNCs). Among the various types of metallic matrices being used, the Al7075 aluminum alloy (a zinc/magnesium/copper alloy) is central to high-stress engineers because of its ultimate tensile strength [14]. One problem with Al7075 is that it tends to grain coarsen through thermal cycles and has limited wear resistance [6,10,14]. To overcome these limitations, the incorporation of bio-derived NAC represents an innovative solution. Unlike synthetic carbon nanotubes (CNTs) and graphene which are incredibly expensive and very much prone to "agglomeration" as a result of extremely high Van der Waals forces, the "NAC" derived from biomass source materials (such as cottons carpel) presents a sustainable, low-cost alternative source material [15-17]. It possesses uniquely functional surface groups that will enhance the "wettability" of the carbon particles in the molten aluminum matrix, a critical characteristic that is required for creating a defect free interface [16]. There are many different micromechanism processes that influence the degree of improvement of the mechanical properties of alloy Al7075 as a result of the reinforcement by using NAC [14]. The "Orowan Strengthening" mechanism described by Ramanathan et al. [5] occurs with the fine dispersion of NAC particles acting as impenetrable barriers to the motion of dislocations, forcing dislocations to bow around the NAC particles thus increasing the yield strength [17-19]. Idrisi et al. [6] demonstrated that biochar nanoparticles effectively refine grain size through "Zener pinning" by restricting the migration of grain boundaries at these locations. The potential of this technology lies in the ability to "tailor" the microstructural characteristics of alloys using extremely precise control of the concentration of the nano-filler [15]. Successful fabrication, on the other hand, is dependent on the meticulous care used in the control of the methods of additions, such as ultrasonic-assisted stir casting or powder metallurgy (PM), so that no brittle phases (e.g., Al_4C_3) are developed as a result of additions [20]. According to Basavarajappa et al. [7], solid state type processing is superior for controlling the structural integrity of nanoparticles within alloy matrices. While many studies have been conducted on the individual aspects of carbon extraction and metallurgy, there is a profound shortage of accumulated research regarding NACs derived from the cotton carpel material for improvement of Al7075 [21-24]. The cotton carpel, which is very abundant in agricultural regions such as Iraq, contains a very unique lignocellulosic structure that contains very high porosity when activated. The combination of the high strength of Al7075 and sustainable NAC is a significant area of opportunity yet to be examined [25-27]. The research gap is widened by the need to provide a complete evaluation of the effect of NAC on the transition from ductile to brittle failure modes. Therefore, a major goal of this analysis is to formally establish a robust, green-synthesis process for the extraction of NAC from waste materials generated by cotton carpels, as well as to understand how the inclusion of the NAC will affect the microstructural development, hardness, and tensile properties of Al7075. Ultimately, this research will assist in providing sustainable solutions to the production of next generation aluminum-based nanocomposites through valorization of agricultural waste materials, thus achieving sustainable global and advanced manufacturing excellence results.

MATERIALS AND METHODS

MATERIALS SELECTION AND SPECIFICATIONS

7075 aluminum (Al-Zn-Mg-Cu system) was utilized as the main metal for manufacturing the metal matrix. The chemical composition of the Al7075-T6 alloy can be seen in Table 1. The cotton-carpel waste (CCW) used in this work was from Iraq. All the chemicals used in the study, such as NaOH and HCl, were from Sigma-Aldrich (Schnelldorf, Germany). All solutions and rinses used in the study were prepared using de-ionized water.

Table 1. Chemical composition of as-received Al7075-T6 alloy.

Element	Al	Zn	Mg	Cu	Cr	Fe	Si	Mn	Ti	Others (Total)
Composition (Range in %)	Remainder (Balance)	5.1 - 6.1	2.1 - 2.9	1.2 - 2.0	0.18 - 0.28	Max~0.50	Max~0.40	Max~0.30	Max~0.20	Max~0.15
Typical Value%	90.0	5.6	2.5	1.6	0.23	0.20	0.15	0.10	0.05	0.05

EXTRACTION OF NANO-ACTIVATED CARBON (NAC)

A thermochemical multi-stage process has been developed for converting agricultural waste to produce Nano-Activated Carbon (NAC) using agricultural raw materials (CCW from cotton carpels), such as shown in Fig. 1. The process begins with the removal of impurities from the raw material before thermochemical transformation, which requires both cleaning and drying of the raw material. The first step in this process is to chemically purify the raw material by soaking it in hot distilled water for a period of

*Corresponding author
Ruaa A. Salman,
College of Biomedical Engineering, University of Technology-Iraq
e-mail: 70153@uotechnology.edu.iq

time to remove surface impurities and dust before proceeding to the next steps of pre-treatment and pulverization of the material. After the initial cleaning, the raw material is dehydrated in a laboratory oven at 105° C for 24 hours to remove the moisture that is present within the biomass. After the removal of internal moisture, the material is then ground using mechanical means to produce a uniform particle size of approximately 425 µm. After grinding the material, it is carbonized (pyrolyzed) under a nitrogen atmosphere using an electric muffle furnace. The material is carbonized at three different temperatures (250°C, 270°C, and 300°C) using nitrogen gas as the heating medium. The total time for the carbonization and activation process is 30 minutes for producing raw black carbon (BC). The BC is subsequently activated using a two-step process: First, the BC is impregnated with two molar equivalents of sodium hydroxide (NaOH) in a temperature range of 90 to 100°C for 24 hours, and then it is activated by re-carbonizing it in a stainless-steel crucible using a nitrogen atmosphere at 500°C for three hours, with a heating ramp of 5°C/min. The second stage of the activation process uses an acid wash and neutralization step to activate the carbon and remove any inorganic impurities contained within the activated carbon. The BC is treated with 3M hydrochloric acid (HCl) at a temperature of 50°C for three hours and then filtered and rinsed several times with hot distilled water to produce a pH of 7.0 in the filtrate. The final step in producing activated carbon is to dry the activated carbon in a laboratory oven using an nitrogen gas atmosphere at a temperature of 60°C to prevent the presence of oxidizing agents in order to produce a stable porous structure.

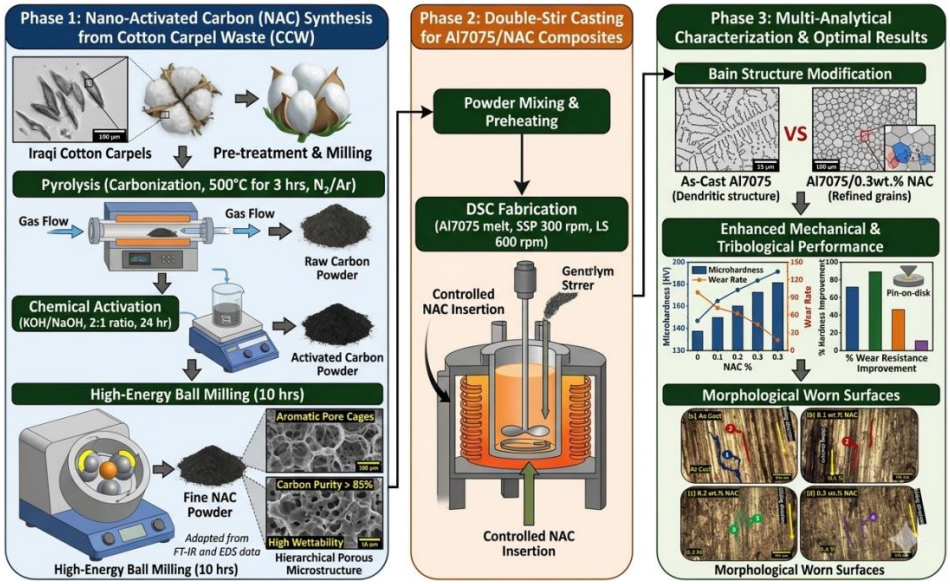

Fig. 1. Flow chart for preparation of the high purity activate nano-powder using precipitation method.

FABRICATION OF AL7075/NAC COMPOSITES

Aluminum matrix composites (AMCs) were produced via a double stir casting method (liquid-state process) for their proven effectiveness in creating uniform distributions of particle sizes. Solid Al7075-T6 rods (50 mm diameter) were chopped to produce appropriately sized feedstock and then added to the high-purity alumina crucible. An electric resistance furnace was then used to melt the feedstock. The fabrication sequence is as follows:

1. Melting and Homogenization: Approximately 250 g of Al7075 was melted at 780 °C (above its liquidus of 650 °C) to ensure that the melt would be purely liquid. The melt temperature was held constant for 15 minutes, at which point 0.2 wt.% of pure magnesium (Mg) was added to assist with wetting of the NAC and to reduce the surface tension at the interface between the aluminum melt and the NAC.
2. Semi-Solid Inclusion: The melting temperature was then reduced to 600 °C, which created a semi-solid state for the aluminum alloy, thus enabling the efficient entrapment of the NAC particles (heated to 400 °C and wrapped in aluminum foil) without allowing them to float to the surface or segregate within the melt. The NAC was added at an average rate of 0.01-0.05 g/s.
3. Double Stirring Mechanism: A low-speed stirring phase was initiated in the semi-solid state at 350 rpm for 12 minutes. The temperature was then increased back to the fully liquid state (with an additional 20 °C added for cooling due to the stirring operation) using an argon gas shroud. A second high-speed stirring phase was then initiated at 600 rpm for 13 minutes, which should provide sufficient shear to fragment any remaining clusters and provide a globally uniform distribution.
4. Casting: After the slag was removed (using a specific de-slagging flux), the composite material was poured into a split die made of medium-carbon steel (PRE-HEATED TO 300 °C), which contained two cavities (20 mm x 60 mm). Specimens were allowed to solidify at room temperature to ensure the presence of a refined dendritic structure. The experimental design included a (four) composition matrix, as identified in Table 2.

*Corresponding author
Ruaa A. Salman,
College of Biomedical Engineering, University of Technology-Iraq
e-mail: 70153@uotechnology.edu.iq

Table 2. Composition of the fabricated specimens for the Al7075 alloy.

Specimen ID	Reinforcement (NAC) Concentration (wt.%)
S0	0.0
S1	0.2
S2	0.4
S3	0.6

MECHANICAL AND MICROSTRUCTURAL CHARACTERIZATION

To evaluate the impact of NAC reinforcement on the Al7075 matrix, the cast samples were subjected to rigorous metallurgical and mechanical assessments. Specimens (10 mm \times 10 mm) were sectioned from the castings and prepared via standard metallographic procedures (grinding and polishing). Etching was performed to reveal grain boundaries. The surface morphology and elemental distribution were analyzed using scanning electron microscopy (SEM) coupled with energy-dispersive spectroscopy (EDS). Vickers microhardness tests were conducted in accordance with ASTM E384 using a Mitutoya MVK-H1 tester. A load of 300 g was applied for a dwell time of 10 seconds. To ensure statistical reliability, measurements were taken at three different regions for each specimen, and the Vickers Hardness Number (HV) was determined using the following relation:

$$HV = \frac{1.854 \times P}{d^2} \quad (1)$$

where P is the applied load (kg) and d is the average diagonal length of the indentation (mm).

The tribological behavior was assessed using a Pin-on-Disk apparatus following the ASTM G99 standard. Cylindrical pins (10 mm diameter, 20 mm height) were rubbed against a hardened steel disk (35 HRC) under the following conditions:

- Loads: 5, 10, and 15 N.
- Sliding Speed: 2.8 m/s (490 rpm).
- Sliding Time: 15 minutes.

According to ASTM G99 the wear rate (WR) was calculated by measuring the difference in weight before and after the test (in grams g) (ΔW) and applying the formula:

$$WR = \frac{\Delta W}{\pi \times D \times N \times t} \quad (2)$$

Diameter of the Sliding Circle (D) = Sliding Circle Diameter (D) Rotational Speed (N) = Rotational Speed (N) Time for Test (t) = Time for Test (t) Each test was perfromed in triplicate to validate repeatability and the wear surfaces were evaluated by SEM to assess prevailing wear mechanisms (e.g. Abrasive, Adhesive or Delaminating).

$$Improvement(\%) = \frac{WR_{base} - WR_{modified}}{WR_{base}} \times 100 \quad (3)$$

where WR_{base}, Represents the control sample. and $WR_{modified}$ represents the improved sample (composite).

RESULTS AND DISCUSSION

EXTRACTED NANO-ACTIVATED CARBON (NAC)

The method used for producing functional carbon materials from agricultural residues is highly dependent on their intrinsic properties. Properties are directly related to the original composition of the biomass. In Table 3, a summary of the component parts of the ICC (Iraqi Cotton Carpel) is provided. Due to high levels of cellulose and holocellulose, the ICC is an ideal raw material to produce carbon materials with an extensive aromatic structure. Since 31% of lignin is also present, its ability to provide a high carbon yield during the carbonization process is due in large part to its hierarchical chemical structure which makes it resistant to complete thermal degradation.

Table 3. Chemical composition of the raw cotton carpel biomass.

Composition (wt.%)	Properties
44.50	alpha-Cellulose
72.30	Holocellulose
31.00	Lignin
4.20	Extractives
1.60	Ash Content

The absorbance profiles shown in Fig, 2 change drastically compared to low-frequency ranges; likewise, the complexity of functional groups at the surface, along with their thermal stability, evolves from rich and complex at 5000–4000 cm^{-1} for the FT-IR transmittance sample spectra presented in Fig. 2 (points S1 and S2) with no significant presence of structural impurities—such as surficial moisture present in S3—based upon structural and functional character data from S1. The peaks from each of the three samples at approximately 3377 cm^{-1} correspond to the hydroxyl stretching vibrations of —OH functional groups generally accepted to be derived from moisture adsorbed to the surface of AC as well as from the structural-based —OH functional groups present in phenolic and carboxylic structural species developed during the thermal degradation of wood. The presence of the compound-type C=C stretching at approximately 2369 cm−1 corresponds to the cumulative double bonds (compounds) produced by the decomposition of lignin–cellulose prior to the char (compounds that are characteristic of the carbonization of

*Corresponding author
Ruaa A. Salman,
College of Biomedical Engineering, University of Technology-Iraq
e-mail: 70153@uotechnology.edu.iq

cellulose/lignin), which could have developed at the same time as the other carbon forms during the decomposition process. The primary structural and functional character of the compounds in this fingerprint region (2000–1000 cm^{-1}) are partially represented in their developing new peaks beginning at approximately 1597–1602 cm^{-1}, which correspond to the skeletal C=C stretching of aromatic structure and the skeletal C=O stretching of carbon-based conjugated C=O functional groups; consequently, S3 has developed significant amounts of stable carbon materials with respect to their carbonization temperature. The presence of a developing/fairly broad peak in the region of 1202–1212 cm^{-1} that is related to the C-O stretching of ether/epoxy and phenolic groups affirms that the functionalization of oxygen to stable carbon has, through the processes discussed, been achieved through progressive increases in carbonization temperature. Apart from the changes that occur at the identified peaks due to increases in the carbonization temperatures of S1, S2 and S3, the overall changes that occur as a result of the changes from the S1, S2 broad/complex peaks to concentrated/precise peaks at S3 are a good indication of the extent of the changes made to the structural and functional character of the porous media and the formation of stable C-O functional environments through these carbonization temperatures. Hence, each of the identified peaks at S3 develops into very precise/accurate small peaking-type regions with respect to the peaks found on the FT-IR spectra taken for S1, and S2.

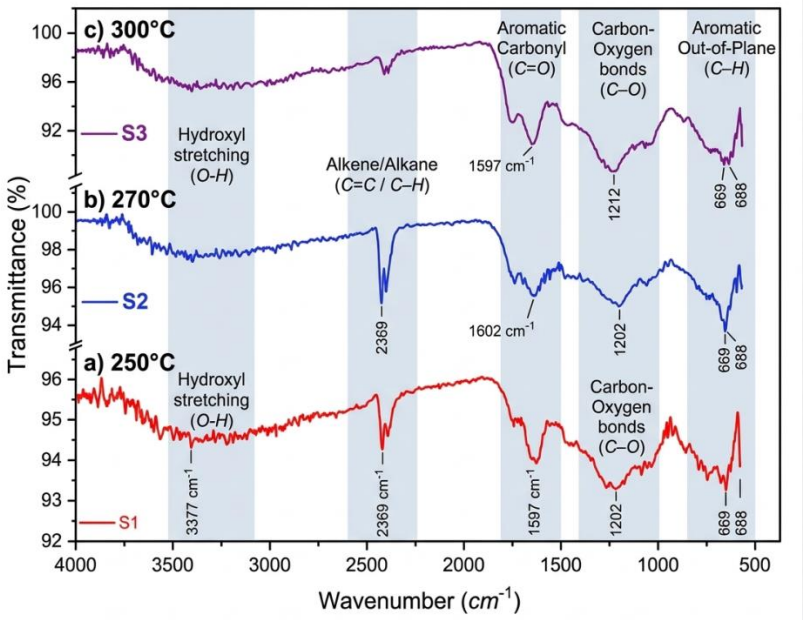

Fig. 2. Stacked FT-IR spectra of NAC extracted from cotton carpel waste, illustrating the evolution of surface functional groups as a function of carbonization temperature: a) 250°C, b) 270°C, and c) 300°C.

The elemental content is indicated by the comparative element dispersive X-ray spectroscopy (EDS) spectrum in Fig. 3. Analyzing the different carbonization temperatures of the NAC produced from cotton carpal waste indicates observable changes based upon the amount of carbon (C) and oxygen (O) present. All three samples had distinct peaks associated with carbon (C) and exhibited similar increases in peak intensity as carbonization temperature increased, with sample c (NAC produced at 300°C) having the most peaks on the spectrum due to the carbonization of the material. In all three samples, the peak was associated with the production of carbon due to the high levels of carbon and weight percent produced during carbonization. The second most prevalent peak was associated with oxygen (O) for all three samples. The sample with the highest intensity of oxygen was produced at 250 °C and will also contain residual structural water, organic functional groups, and/or nitrogen (N) based on prior FT-IR analysis (as previously referenced). The presence of these high levels of oxygen in the material may improve the wettability of derived nano-activated carbon (NAC, derived from AC) within the Al7075 matrix, subsequently enhancing bonding between the Al7075 matrix and NAC. The secondary elements potassium (K), calcium (Ca), and sodium (Na) on the EDS spectrum were also detected present at different concentrations, likely residuals from chemical agents used to activate the AC during the experimental procedure or naturally found as minerals within shredded cotton carpal biomass. The trace elements detected were minimal, demonstrating the purification and HCl washing process to remove metallic impurities from the carbonaceous materials prior to the production of the Al7075/NAC-reinforced composite materials was effective. The overall evidence indicates the successful conversion of Iraqi cotton carpal waste to high-grade carbonaceous material can be achieved through the modified carbonization process at 300 °C for producing high-purity carbon, maximizing carbon yield, and providing the potential for reinforcing high-strength aluminum composite alloys.

*Corresponding author
Ruaa A. Salman,
College of Biomedical Engineering, University of Technology-Iraq
e-mail: 70153@uotechnology.edu.iq

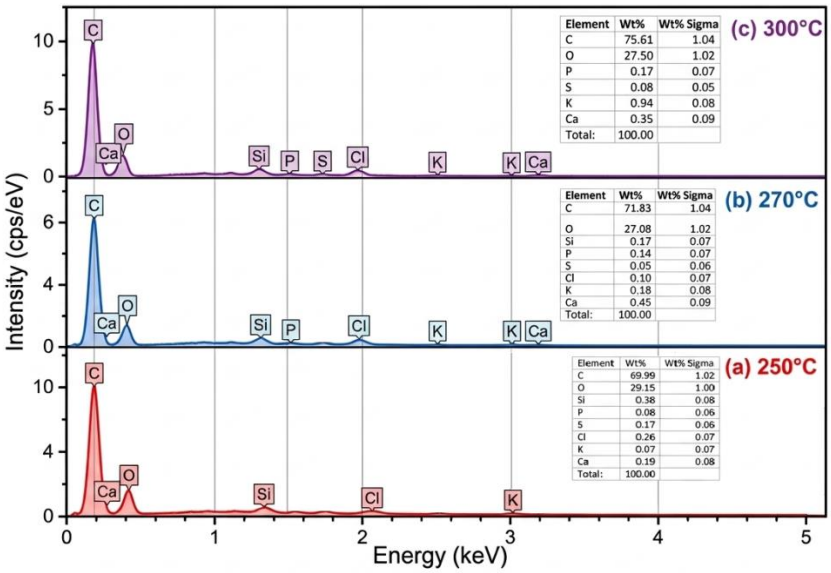

Fig. 3. Comparative Energy-Dispersive X-ray Spectroscopy (EDS) spectra of Nano-Activated Carbon (NAC) extracted from cotton carpel waste, illustrating the evolution of elemental composition as a function of carbonization temperature: a) 250°C, b) 270°C, and c) 300°C.

FE-SEM MORPHOLOGICAL AND POROUS STRUCTURE ANALYSIS

Field emission scanning electron micrographs as a comparison (Fig. 4) depict three different carbonization process temperatures with respect to each of the individual characteristics for each of the products made. e.g., 250°C produced a final product that still contained many of the original forms of the cotton carpel, as illustrated in Fig. 4-a, but at the same time numerous micropores and mesopores and huge numbers of longer pores (macropores or voids). For example, at 250°C, there were a large number of irregularly shaped cantaloupe (lobe) structures in the original material, typical of plant-based chars. In fact, with respect to the 250°C product, it can be characterized by a high surface area with a high roughness or number of surface areas available to absorb (i.e., provide "active" absorption sites for the absorption of molecules). Furthermore, numerous irregular features appear within the pores visible on the product (e.g., micrometer cavities) with a width to depth ratio (w/d) less than 2 (i.e., < 2 nm) and provide a large network throughout the entire material for w/d > 2 (i.e., mesopores) to transport through the layer made up of multiple layers within 1 material type at the same time. The irregular structures that are built upon each material surface, as well as many light-colored objects present, are indicative of incomplete decomposition and the presence of minerals (e.g., Ca & SiO_2 are both found in the cotton carpel) that have an effect on absorption. Once at the carbonization temperature of 270°C, there were signs of a weakened structure and an increasing number of larger pores or channels (macropores) formed throughout the material, as illustrated in Fig. 4-b, but many residual structures contain remnants of the original plant structure, such as fibrous bundles. The temperature of 300°C illustrated in Fig. 4-C is representative of the greatest degree of structure development present and most fragmented product possible. The micrograph illustrates a highly fragmented and fractured surface as well as voids or "Aromatic Pore Cages" within the structure of the material. Furthermore, the reduction in oxygen during the thermal process (as evidenced by EDS results) at the carbonization temperature of 300°C was indicative of the thermal breakdown of cotton carpel biomass into pure, stable, aromatic structures. Due to the high degree of purity of NAC with carbonization temperatures at 300°C, the NAC produced using this biomass will perform comparably to NAC derived from non-renewable feedstocks.

*Corresponding author
Ruaa A. Salman,
College of Biomedical Engineering, University of Technology-Iraq
e-mail: 70153@uotechnology.edu.iq

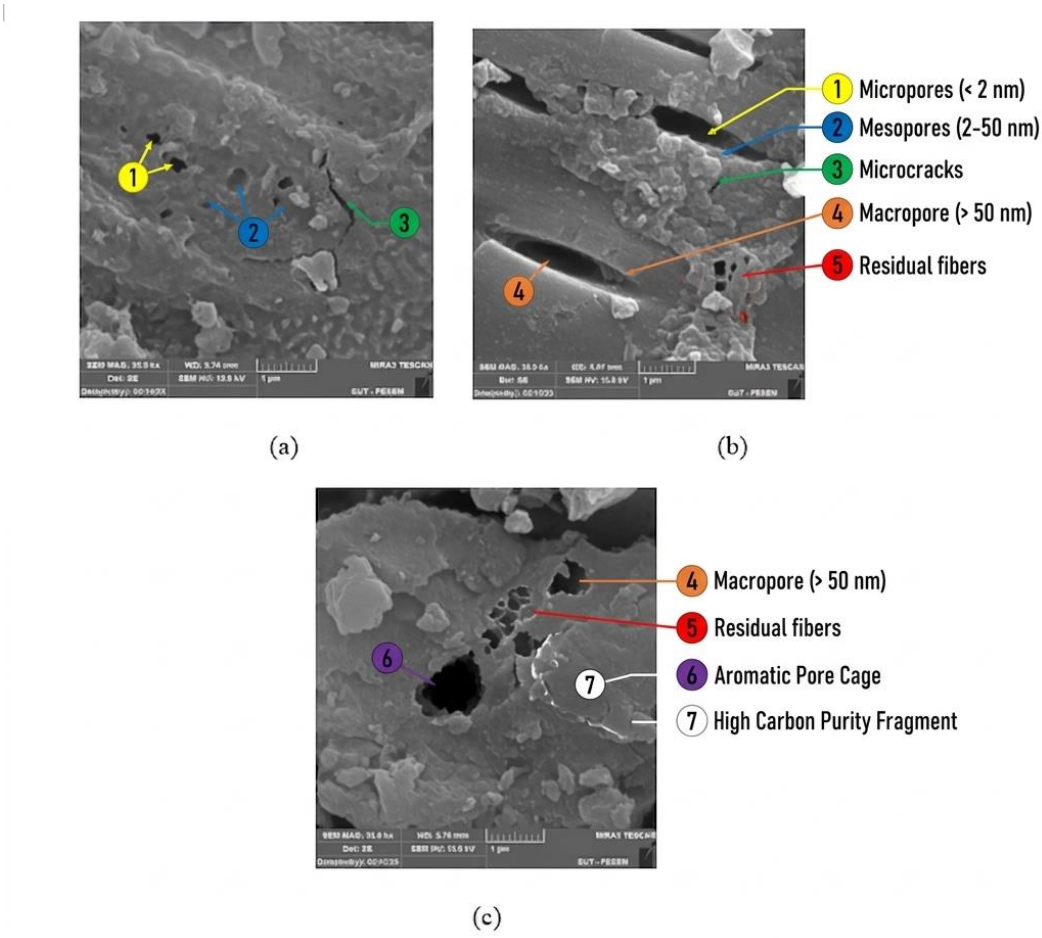

Fig. 4. FE-SEM micrograph of nano-activated carbon (NAC) extracted from cotton carpel waste, illustrating the evolution of surface morphology and porous structure as a function of carbonization temperature: a) 250°C (S1), b) 270°C (S2), and c) 300°C (S3).

CHARACTERIZATION OF AL7075-BASED ALUMINUM MATRIX NANOCOMPOSITES (AMNCS)

OPTICAL MICROSTRUCTURE OF AL7075/NAC COMPOSITES

An examination of the optical microstructure (Fig. 5) provides critical knowledge of how importing extracted nano-activated carbon (NAC) into a high-strength Al7075 aluminum alloy will help create a mechanism through which fine-grained structures are produced.

As cast Al7075 (0.0 wt% NAC): The microstructure of the base alloy as cast (Fig. 5-a) displayed a large, coarse dendritic structure, which is representative of conventional solidification processes within non-modified metallic matrices. The unrefined casting process typically produces slow cooling rates, which allow the unrestricted growth of the long, branched dendrites. This large grain size exhibits few grain boundaries, thereby providing little resistance to dislocation motion, ultimately resulting in a lower level of Vickers hardness of the as-cast samples.

0.1 wt% NAC (S1): As soon as the smallest amount (~0.1 wt%) of NAC was added, structural changes became visible (Fig. 5-b). The NAC nanoparticles act as effective heterogeneous nucleation sites while in the molten state of the composite material. The result of this is the reduction in the energy necessary to form a crystal, which promotes the rapid formation of new, small grains that restrict the excessive growth of existing dendritic structures. The dendrites are fragmented, in the process of changing to a semi-dendritic state with reduced interdendritic spacing. The increased density of grain boundaries obstructs dislocation gliding, subsequently enhancing hardness.

0.2 to 0.3 wt% NAC Composites (S2 and S3): The effect of NAC on the microstructural refinement becomes more evident with the addition of the higher wt% NAC (~0.2-0.3 wt%). The gradual tendency towards refinement is clearly visible throughout the matrix, indicating development of a fine equiaxed grain structure with very little dendritic nature (Fig. 5-c and d). The ultra-fine, homogeneous grain structure will provide the most optimized distribution of the NAC structural elements that will maximize wear strengthening in addition to restricting molecular plowing, which will ultimately lead to a large wear resistance. The uniformity of the microstructure will create new opportunities for broad engineering applications that require high-strength, lightweight nanocomposites.

*Corresponding author
Ruaa A. Salman,
College of Biomedical Engineering, University of Technology-Iraq
e-mail: 70153@uotechnology.edu.iq

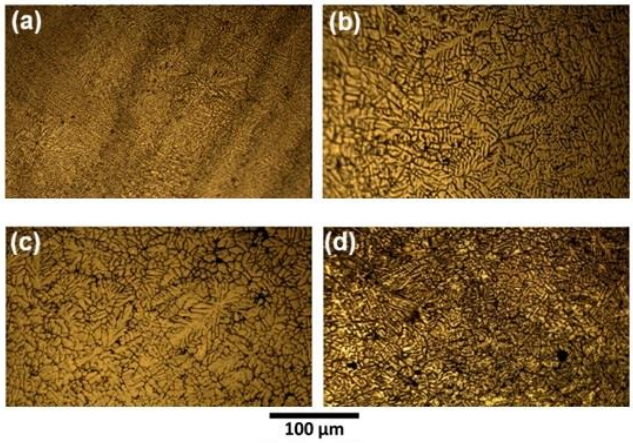

Fig. 5. Comparative Optical Micrographs in Al7075/NAC nanocomposites

MICROHARDNESS AND WEAR MECHANISMS

This study sought to produce Al7075 metal matrix composites (MMCs) through the incorporation of nano-activated carbon (NAC) with varying percentages: 0.1, 0.2, and 0.3 wt% as shown in Fig. 6, and Table 4. The NAC percentages were determined based on previous optimization trials that had been completed in order to minimize the amount of interface or agglomeration within the MMC and maintain the structural integrity of the resulting composite, while also ensuring homogeneity. The principle barrier to the success of this project was the incorporation of the NPs, as they had a very large specific surface area; therefore, if the addition of NPs were greater than 0.3 wt%, the distribution of the NPs would be unevenly distributed within the Al7075 matrix. Thus, in order to achieve a homogeneous distribution of NPs within the Al7075 matrix, a novel double stir casting (DSC) method of preparation was utilized. The greatest enhancement in microstructure of the Al7075 matrix and the resulting mechanical and tribological properties were observed for the 0.3 wt% (S3) composite; Vickers microhardness increased from 130.0 HV for the unreinforced matrix to 164.8 HV. In addition, the average wear rates of all loads (5, 10, and 15 N) decreased with increments in NAC content from 0.1 to 0.3 wt%; for the 15 N applied load, the wear resistance of the S3 composite was improved by 90.72% over that of the Al7075 matrix. Furthermore, for the 15 N applied loads of S3 and all other composite samples, the wear rates converged into the 'mild wear' regime. Moreover, NAC NPs were critical to the development of a robust and durable tribo-layer, thereby reducing or mitigating the metal-to-metal contact and thermal softening that occurred with slippage and increasing the load-bearing properties and structural integrity of the resulting nanocomposite.

Table 4. Wear rate analysis and percentage improvement of Al7075/NAC composites

NAC Content (wt.%)	Vickers Hardness (HV)	Load (N)	Average Wear Rate (10−6 g/cm)	Improvement(%)
As-Cast(0.0)	130.0	5	0.804815	—
		10	1.951431	—
		15	2.924836	—
S1(0.1)	152.5	5	0.500948	37.76
		10	0.978823	49.84
		15	1.560480	46.65
S2(0.2)	155.5	5	0.315673	60.78
		10	0.513079	73.71
		15	0.808359	72.36
S3(0.3)	164.8	5	0.214173	73.39
		10	0.319921	83.61
		15	0.271502	90.72

*Corresponding author
Ruaa A. Salman,
College of Biomedical Engineering, University of Technology-Iraq
e-mail: 70153@uotechnology.edu.iq

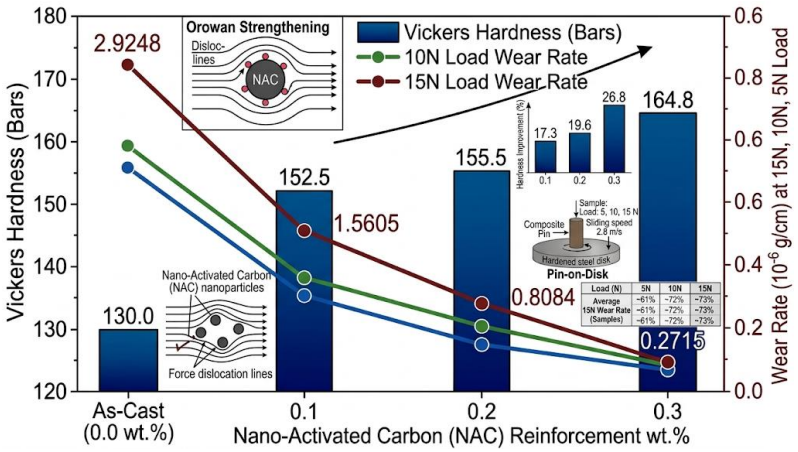

Fig. 6. Comparative evolution of Vickers microhardness and wear rate of Al7075/NAC nanocomposites as a function of reinforcement weight fraction (0.1, 0.2, and 0.3 wt.%).

Microstructural analysis of the wear surfaces, as shown in Fig. 7 reveals a major change in the tribological performance of the Al7075 matrix resulting from the addition of waste-derived nanocarbon (NAC) reinforcements. The as-cast alloy displays only a little evidence of multiple types of wear due to the very large depths of plowing grooves and a great degree of delamination caused by the fact that its coarse dendritic structure cannot resist plastic deformation. The first addition of 0.1 wt% NAC to the alloy results in a significant refinement in grain size of the alloy and, therefore, reduces the extent of damage at the surface. As more NAC is added to the alloy (0.2 to 0.3 wt%), the grade and porous architecture of the NAC derived from Iraqi cotton carpels enhances interfacial bonding and enhances Orowan strengthening, resulting in a shift from severe abrasive wear to mild micro-grooving. The composite with the highest concentration (0.3 wt% NAC) exhibits the best characteristics of any of the comengd composites, as evidenced by the relatively smooth, refined nature of its surface and the highest microhardness (approximately 164.8 HV) and lowest wear rate (approximately 0.2715 x 10^{-6} g/cm). These findings demonstrate that the appropriate concentration of NAC (0.3 wt%) will provide significant improvements in the load bearing and wear resistance of the Al7075/NAC nanocomposites making them excellent candidates for applications in high-performance engineering.

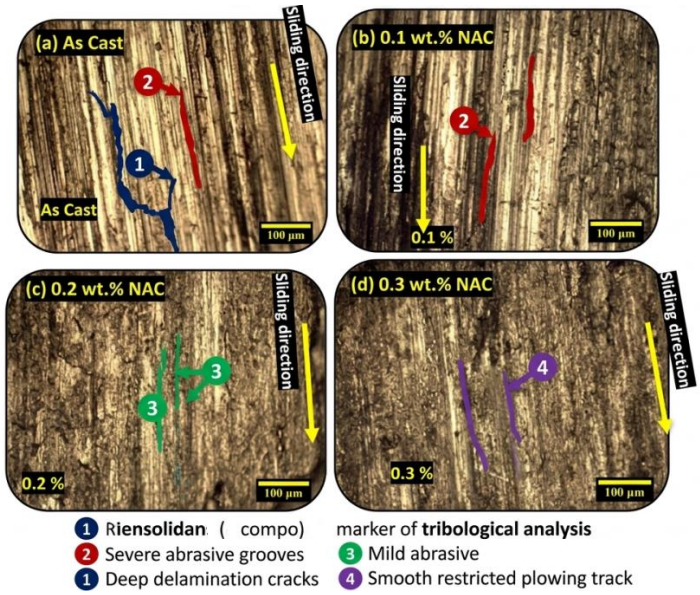

Fig. 7. Integrated morphological analysis of wear rate of Al7075/NAC nanocomposites.

CONCLUSIONS

1. This study successfully examined the mechanical and tribological behavior of the Al7075 alloy reinforced with various weight percentages of nano-activated carbon (NAC). The most significant achievement of this research was the successful synthesis and extraction of high-purity nanocarbons from renewable plant-based biomass as well as confirming a green thermochemical method for producing high-value functionalized nano-reinforcements from low-value biomass. Based on the experimental results and synthesised analytical data from the study, the following conclusions were reached:
2. Mechanical Strengthening. The incorporation of extracted NAC nanoparticles into Al7075 greatly enhanced the matrix's microhardness properties. The maximum Vickers hardness measured for the 0.3 wt.% NAC composite (Sample S3) was 164.8 HV

*Corresponding author
Ruaa A. Salman,
College of Biomedical Engineering, University of Technology-Iraq
e-mail: 70153@uotechnology.edu.iq

compared to 130.0 HV for the as-cast alloy, demonstrating a significant enhancement possible due in part to the capacity of NAC particles to create dislocation pinning (via wear-strengthening mechanism) of the Al7075 matrix.

3. Wear Resistance Optimization. An inverse relationship was discovered between hardness and wear rate. The bio-derived NAC significantly reduced average wear rates at all applied loads (5N, 10N, and 15N) compared to all composites. The highest wear resistance was delivered by the 0.3 wt.% NAC Composite (S3) at an improvement rate of 90.72% when subjected to 15N applied load.

4. Morphological Transformation. Optical microscopy created images of wear surfaces that indicated a change to the wear mechanism between both the as-cast alloy (characterized by significant delamination and deep abrasive grooves) and NAC-reinforced samples (produced far less damage with smoother surfaces). This result provides support for the ability of NAC particles to create a stable protective barrier during sliding against the Al7075 alloy.

5. Sustainability and Efficiency. The successful transformation of biomass-based NAC into Al7075 produces not only an improvement in the mechanical properties of Al7075 but also provides an alternative to synthetic nanomaterials, creating a sustainable, cost-effective method of achieving a circular economy in the metalworking industry.

REFERENCE

[1] Doke, K. M., & Khan, E. M. (2017). Equilibrium, kinetic and thermodynamic analysis of adsorption of reactive dyes from aqueous solution onto activated carbon prepared from agricultural waste. *Journal of Environmental Management*, 193, 244-252. https://doi.org/10.1016/j.jenvman.2017.02.011

[2] Ahmad, M.A., & Alrozi, R. (2011). Optimization of preparation conditions for mangosteen peel-based activated carbon for the removal of Remazol Brilliant Blue R using response surface methodology. *Chemical Engineering Journal*, 170(1), 152-161. https://doi.org/10.1016/j.cej.2011.03.045

[3] Zhang, H., Mansouri, H., & Gu, J. (2016). Strengthening of aluminum alloys by ball milling with carbon-based nanomaterials: A review on the microstructure and mechanical properties. *Materials & Design*, 94, 452-463. https://doi.org/10.1016/j.matdes.2016.01.032

[4] Spathis, G., & Kontou, E. (2001). Dynamic mechanical properties of carbon black reinforced polymer composites. *Journal of Applied Polymer Science*, 81(4), 934-942. https://doi.org/10.1002/app.1513

[5] Ramanathan, A., Krishnan, P. K., & Muraliraja, R. (2019). A review on the production of metal matrix composites through stir casting – Process variables, seaweed reinforcements, and strengthening mechanisms. *Journal of Magnesium and Alloys*, 7(3), 337-355. https://doi.org/10.1016/j.jma.2019.05.009

[6] Idrisi, A. H., Mourad, A. H., & Al-Marzouqi, A. H. (2021). Microstructure and mechanical performance of Al7075 alloy reinforced with bio-char particles. *Materials Today: Proceedings*, 46, 1234-1240. https://doi.org/10.1016/j.matpr.2021.02.345

[7] Basavarajappa, S., Dinaharan, I., & Paulo Davim, J. (2020). Synthesis and characterization of aluminum matrix composites reinforced with plant-based agricultural waste: A state-of-the-art review. *Journal of Materials Research and Technology*, 9(6), 15412-15435. https://doi.org/10.1016/j.jmrt.2020.11.022

[8] Abdul Khalil, HPS, Noriman, NZ, Ahmad, MN, Ratnam, MM, & Fuaad, NAN (2007). Polyester Composites Filled Carbon Black and Activated Carbon from Bamboo (Gigantochloa scortechinii): Physical and Mechanical Properties. *Journal of Reinforced Plastics and Composites* , 26(3), 305-320. https://doi.org/10.1177/0731684407065066

[9] Koli, A., Pattanshetti, A., Mane-Gavade, S., Dhabbe, R., Kamble, R., Garadkar, K., & Sabale, S. (2024). Agro-waste management through sustainable production of activated carbon for CO2 capture, dye and heavy metal ion remediation. *Waste Management Bulletin* , 2, 97-121. https://doi.org/10.1016/j.wmb.2023.10.001

[10] Wang, Y., Yang, F., Wu, T., & Huang, G. (2024). Systematic overview of the preparation, interface characteristics, strengthening mechanisms, and challenges of graphene-reinforced Al matrix composites. *Journal of Materials Research and Technology*, 33, 7709-7739. https://doi.org/10.1016/j.jmrt.2024.10.015

[11] Abdul Khalil, H. P. S., Firoozian, P., Bakare, I. O., Akil, H. M., & Noor, A. M. (2010). Exploring biomass based carbon black as filler in epoxy composites: Flexural and thermal properties. *Materials & Design* , 31(7), 3419-3425. https://doi.org/10.1016/j.matdes.2010.01.036

[12] Omara, A. E. D., Elsakhawy, T., Alshaal, T., El-Ramady, H., Kovács, Z., & Fári, M. (2019). Nanoparticles: A Novel Approach for Sustainable Agro-Productivity. *Environment, Biodiversity and Soil Security* , 3, 29-62. https://doi.org/10.21608/jenvbs.2019.7478.1050

[13] Abdul Khalil, H. P. S., Jawaid, M., Firoozian, P., Rashid, U., Islam, A., & Akil, H. M. (2013). Activated Carbon from Various Agricultural Wastes by Chemical Activation with KOH: Preparation and Characterization. *Journal of Biobased Materials and Bioenergy* , 7(1), 1-7. https://doi.org/10.1166/jbmb.2013.1252

[14] Chen, L., Jing, J., Zhao, Y., Hou, H., & Zhao, Y. (2024). Semi-Solid Casting Preparation Technology for Graphene-Reinforced Magnesium Matrix Composites. *Proceedings of the 75th World Foundry Congress* , Part 5: Metal Matrix Composite Materials, Deyang, China.

[15] Thulasiraman, A. V., & Ganesapillai, M. (2023). A Systematic Review on the Synthesis of Silicon Carbide: An Alternative Approach to Valorisation of Residual Municipal Solid Waste. *Processes*, 11(1), 283. https://doi.org/10.3390/pr11010283

[16] Fouad, MJ, Abbass, MK, & İnanç, İ. (2025). Manufacture of Self-Lubricating Mechanical Parts from Al-Si Alloy Matrix Hybrid Nanocomposites. *Tribology in Industry* , 47(1), 112-124. https://doi.org/10.24874/ti.1752.09.24.02

[17] Budapanahalli, S.H., Mallur, S.B., Patil, A.Y., Alosaimi, A.M., Khan, A., Hussein, M.A., & Asiri, A.M. (2022). A Tribological Study on the Effect of Reinforcing SiC and Al2O3 in Al7075: Applications for Spur Gears. *Metals*, 12(6), 1028. https://doi.org/10.3390/met12061028

*Corresponding author
Ruaa A. Salman,
College of Biomedical Engineering, University of Technology-Iraq
e-mail: 70153@uotechnology.edu.iq

[18] Wannassi, B., Kanan, M., Hariz, I. B., Assaf, R., Abusaq, Z., Ben Hassen, M., ... & Barham, A. S. (2023). Cotton Spinning Waste as a Microporous Activated Carbon: Application to Remove Sulfur Compounds in a Tunisian Refinery Company. *Sustainability* , 15(1), 654. https://doi.org/10.3390/su15010654
[19] Yu, Z., Gao, Q., Zhang, Y., Wang, D., Nyalala, I., & Chen, K. (2019). Production of Activated Carbon from Sludge and Herb Residue of Traditional Chinese Medicine Industry and Its Application for Methylene Blue Removal. *BioResources* , 14(1), 1333-1349. https://doi.org/10.15376/biores.14.1.1333-1349
[20] Abdulrahim, M., Kiman, S., Grema, A. S., Gutti, B., & Abubakar, A. M. (2023). An Overview on the Development of Activated Carbon from Agricultural Waste Materials. *Journal of Engineering Management and Information Technology* , 1(4), 207-211. https://doi.org/10.61552/JEMIT.2023.04.006
[21] Muhammad, S., Abdul Khalil, H. P. S., Abd Hamid, S., Albadn, Y. M., Suriani, A. B., Kamaruzzaman, S., & Yahya, E. B. (2022). Insights into Agricultural-Waste-Based Nano-Activated Carbon Fabrication and Modifications for Wastewater Treatment Application. *Agriculture* , 12(10), 1737. https://doi.org/10.3390/agriculture12101737
[22] Lütke, S. F., Igansi, A. V., Pegoraro, L., Dotto, G. L., Pinto, L. A., & Cadaval Jr, T. R. S. (2019). Preparation of activated carbon from black wattle bark waste and its application for phenol adsorption. *Journal of Environmental Chemical Engineering* , 7(5), 103396. https://doi.org/10.1016/j.jece.2019.103396
[23] Devaki, M., Divya, M. P., Sangram, V., Ganesan, M., & Vallal, S. (2022). Preparation and characterization of activated carbon from Lantana camera. *The Pharma Innovation Journal* , SP-11(8), 1819-1822. https://doi.org/10.22271/tpi.2022.v11.i8Sa.15000
[24] Nath, P.C., Ojha, A., Debnath, S., Sharma, M., Sridhar, K., Nayak, P.K., & Inbaraj, B.S. (2023). Biogeneration of Valuable Nanomaterials from Agro-Wastes: A Comprehensive Review. *Agronomy* , 13(2), 561. https://doi.org/10.3390/agronomy13020561
[25] Abebaw, G., Bewket, B., & Getahun, S. (2021). Experimental Investigation on Effect of Partial Replacement of Cement with Bamboo Leaf Ash on Concrete Property. *Advances in Civil Engineering* , 2021, 6468444. https://doi.org/10.1155/2021/6468444
[26] Bagherzadeh, M., Aslibeiki, B., & Arsalani, N. (2023). Preparation of Fe3O4 vine shoots derived activated carbon nanocomposite for improved removal of Cr(VI) from aqueous solutions. *Scientific Reports* , 13, 3960. https://doi.org/10.1038/s41598-023-31015-x
[27] Egun, I. L., He, H., Hu, D., & Chen, G. Z. (2022). Molten Salt Carbonization and Activation of Biomass to Functional Biocarbon. *Advanced Sustainable Systems* , 6(11), 2200294. https://doi.org/10.1002/adsu.202200294

*Corresponding author
Ruaa A. Salman,
College of Biomedical Engineering, University of Technology-Iraq
e-mail: 70153@uotechnology.edu.iq